

Highlights from STAR

Kai Schweda for the STAR collaboration[‡]

E-mail: koschweda@lbl.gov

Lawrence Berkeley National Laboratory, One Cyclotron Rd MS70R0319, Berkeley, CA 94720, USA

Abstract. Selected results from the STAR collaboration are presented. We focus on recent results on jet-like correlations, nuclear modification factors of identified hadrons, elliptic flow of multi-strange baryons Ξ and Ω , and resonance yields. First measurements of open charm production at RHIC are presented.

Submitted to: *J. Phys. G: Nucl. Phys.*

1. Introduction

The ultimate goal of ultra-relativistic nuclear collisions at RHIC is to identify and study matter with partonic – quark and gluon – degrees of freedom. To address this important question, we study

- nuclear effects at intermediate and high transverse momentum p_T to probe initial conditions and potentially partonic energy loss,
- bulk properties of matter to probe the collisions dynamics, to detect collective motion among partons and finally to determine the equation of state of partonic matter.

STAR also has an active program on ultra-peripheral collisions, where the Au nuclei interact only via the long range electromagnetic force [1]. In collisions with polarized protons, we investigate the spin structure of the nucleon [2].

This paper is structured as follows. Section 2 discusses one example of ultra-peripheral collisions. I will then exclusively focus on ultra-relativistic nuclear collisions. In Sec. 3, recent results on jet-like correlations and nuclear modification factors at intermediate and high p_T are presented. Azimuthal anisotropy parameters are shown in Sec. 4. Section 5 discusses particle production and bulk properties. Section 6 presents first measurements on open charm production at RHIC.

[‡] see appendix for author list

2. Ultra-peripheral collisions

In ultra-peripheral collisions, the Au nuclei interact only via the long range electromagnetic force. Vector mesons are produced when a photon from the electromagnetic field of one Au nucleus strikes the other one. Production can occur at either nucleus; the two possibilities interfere destructively, reducing production at small p_T [3]. Figure 2 shows the raw $t_\perp = p_T^2$ spectrum for ρ^0 photoproduction in $0.1 < |y| < 0.5$ from Au+Au collisions at $\sqrt{s_{NN}}=200$ GeV. STAR data (points) are compared with calculations with and without the interference. The data drops at small p_T , showing that there is interference between ρ^0 photoproduction at two well-separated nuclei.

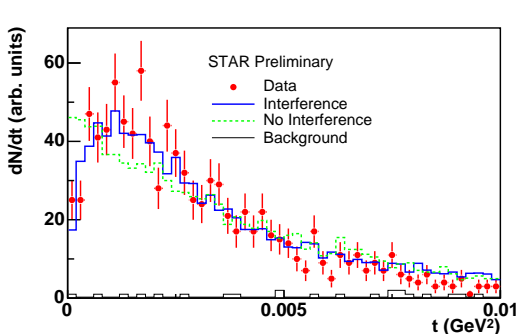


Figure 1. Raw spectrum for ρ^0 sample at $0.1 < |y| < 0.5$ from ultra-relativistic Au+Au collisions at $\sqrt{s_{NN}}=200$ GeV. The points show our experimental results. The solid histogram are results from calculations incorporating coherent ρ^0 production, while the dashed histogram shows results from simulations without interference. The solid histogram with very few counts displays the background contribution.

3. Measurements at intermediate and high p_T

High transverse momentum hadrons provide an excellent probe of the high energy density matter created at RHIC [4]. The measurement of particle yields and jet-like correlations at intermediate and high p_T have demonstrated that indeed a hot and dense medium is created in Au+Au collisions at RHIC [5, 6, 7, 8]. The solid line in figure 2(a) shows the azimuthal distribution of charged hadrons at $2 \text{ GeV}/c < p_T < p_T^{\text{trig}}$ with respect to a trigger particle with $4 < p_T^{\text{trig}} < 6 \text{ GeV}/c$ for $p + p$ collisions at $\sqrt{s_{NN}}=200$ GeV. This distribution exhibits an enhancement around $\Delta\phi \sim 0$ which is typical of jet production, and around $\Delta\phi \sim \pi$ typical of di-jet events.

On the other hand, azimuthal distributions from mid-central Au+Au collisions for particles within the reaction plane ($|\phi| < \pi/4$) and out-of the reaction plane ($|\phi| > \pi/4$) are shown by squares and circles, respectively [9]. Contributions from elliptic flow and pedestals have been subtracted. Here, ϕ is the particle angle with respect to the reaction plane, while $\Delta\phi$ is the particle angle with respect to the trigger particle. To increase statistics, the results from Au+Au collisions are measured for $|\Delta\phi|$ (solid symbols) and were reflected about $|\Delta\phi| = 0$ and $|\Delta\phi| = \pi$ (open symbols). All three distributions exhibit an enhancement in the near-side region. However, the Au+Au results show a relative suppression in the away-side region which is stronger in the out-of-plane direction. The observed suppression is consistent with the jet quenching scenario, where fast partons or their hadronic fragments lose energy due to interactions with the medium created at RHIC. The pathlength in the initial overlap region of both Au nuclei is larger

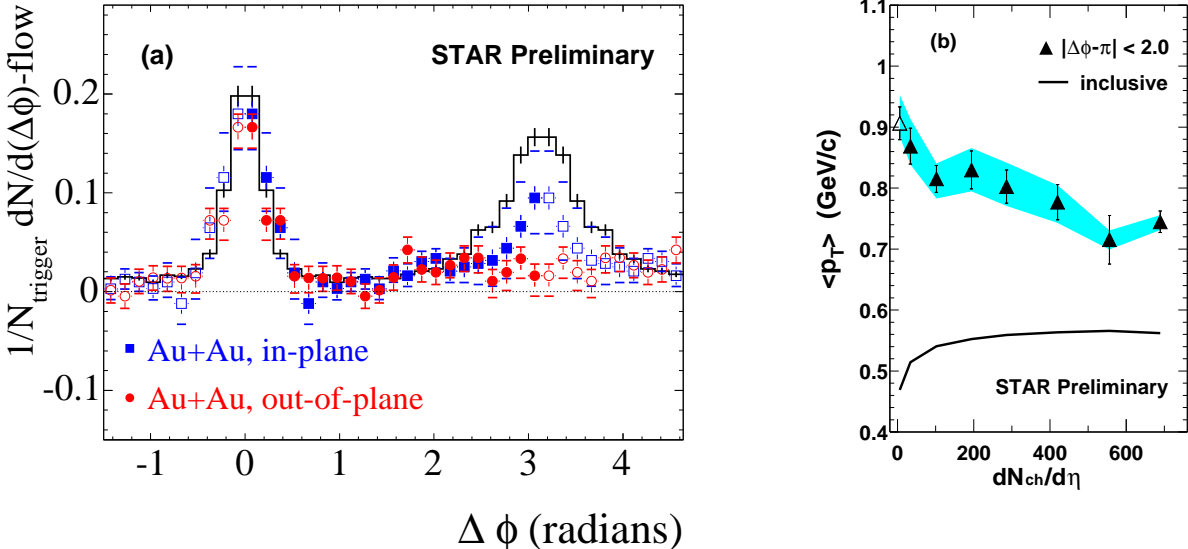


Figure 2. (a) Azimuthal distribution of particles with respect to a trigger particle for $p + p$ -collisions (solid line), and mid-central Au+Au collisions within the reaction plane (squares) and out-of-plane (circles) at $\sqrt{s_{\text{NN}}}=200$ GeV and (b) mean transverse momentum for particles around the away-side region as a function of number of charged particles. The solid line shows the mean transverse momentum of inclusive hadrons.

in the out-of-plane direction than in-plane. Therefore, in the jet-quenching scenario one would expect a larger suppression in the out-of-plane direction which is consistent with our experimental data.

Figure 2(b) shows the mean transverse momentum of charged hadrons with $0.15 < p_T < 4.00$ GeV/c associated with a trigger particle around the away-side region [10] as a function of increasing centrality, as measured by the number of charged particles. The background contribution was determined by an event-mixing technique and has been subtracted. The mean transverse momentum is decreasing with centrality indicating a steady softening of the spectrum in the away-side region. In contrast, the mean transverse momentum of inclusive hadrons is increasing due to the larger amount of transverse radial flow developed in more central collisions. This is shown by the solid line in figure 2(b). The observed softening in the away-side region suggest that energy originally carried by fast partons is largely dissipated in the collision medium.

Besides correlation with respect to a single trigger particle, STAR has measured two-particle correlations locally on $\eta-\phi$ for charged hadrons with $p_T < 2.0$ GeV/c [11]. Even at these relatively small momenta, we observe enhancements in the away-side and same-side region as well as a suppression of the away-side to same-side amplitude ratio as a function of centrality.

Models incorporating initial state parton saturation effects [12] also predict considerable suppression of hadron yields at high p_T . In our d +Au control measurement, where a hot, dense medium is not produced, we do not observe any suppression of yields in the p_T range 2–7 GeV/c [13]. Therefore, our data strongly suggest that the observed suppression in Au+Au collisions is due to interactions in the medium.

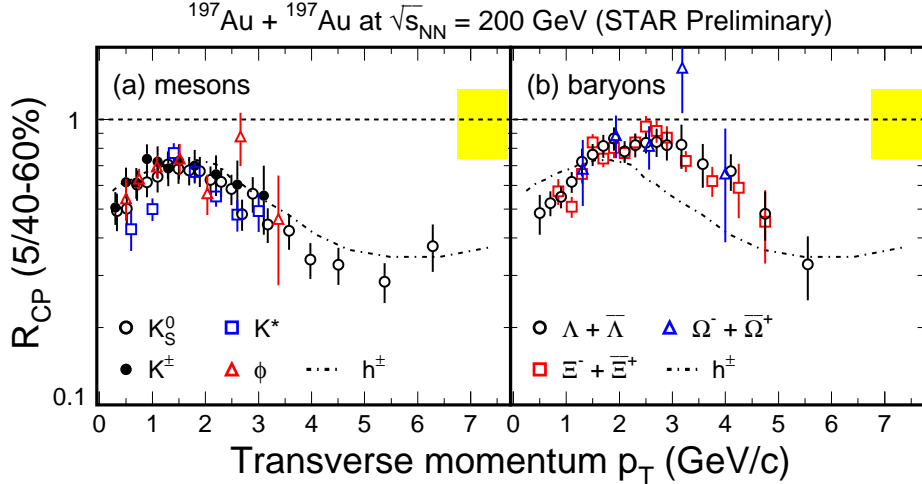


Figure 3. (a) Nuclear modification factors of identified mesons and (b) identified baryons from Au+Au collisions at $\sqrt{s_{NN}}=200$ GeV. The dashed lines show experimental results for charged hadrons. Peripheral Au+Au collisions were used as a reference.

Nuclear modification factors from 5% most central Au+Au collisions at $\sqrt{s_{NN}}=200$ GeV [14, 15, 16] are shown in figure 3 up to $p_T < 7$ GeV/c for (a) identified mesons, namely K_S^0 (open circles), charged kaons (closed circles), K^* (open squares), ϕ (open triangles) and (b) identified baryons Λ and $\bar{\Lambda}$ (open circles), Ξ and $\bar{\Xi}$ (open squares) and Ω and $\bar{\Omega}$ (open triangles). The dashed lines show experimental results for charged hadrons. As a reference, yields from peripheral (40–60%) Au+Au collisions were used. The hatched bands show Glauber model expectations for scaling of the yields with the number of binary collisions ($p_T > 7.0$ GeV/c) and their respective systematic uncertainties. In the intermediate p_T range at $2 < p_T < 6$ GeV/c, there seem to be two groups: Mesons fall into a common band while baryons show consistently larger values. Results for ϕ and $\Omega(\bar{\Omega})$ are still inconclusive due to low statistics.

Quark coalescence or recombination models [17, 18] for hadron formation offer an elegant explanation for the experimentally observed dependence on the number of constituent quarks. Within some of these models [18], hadrons at intermediate p_T are dominantly formed by coalescing quarks stemming from a thermalized parton system, i.e. a quark gluon plasma. Therefore, measurements at intermediate p_T might reveal information on partonic bulk matter.

4. Azimuthal Anisotropy

Azimuthal anisotropy of particle production is sensitive to the early stage of ultra-relativistic nuclear collisions [19, 20]. Figure 4(a) shows measured azimuthal anisotropy parameters v_2 of the strange hadrons K_S^0 (open triangles), Λ and $\bar{\Lambda}$ (open circles), Ξ and $\bar{\Xi}$ (closed circles) and Ω and $\bar{\Omega}$ (closed squares) as a function of transverse momentum p_T for minimum bias Au+Au collisions at $\sqrt{s_{NN}}=200$ GeV [21]. Strange baryons exhibit a significant amount of elliptic flow.

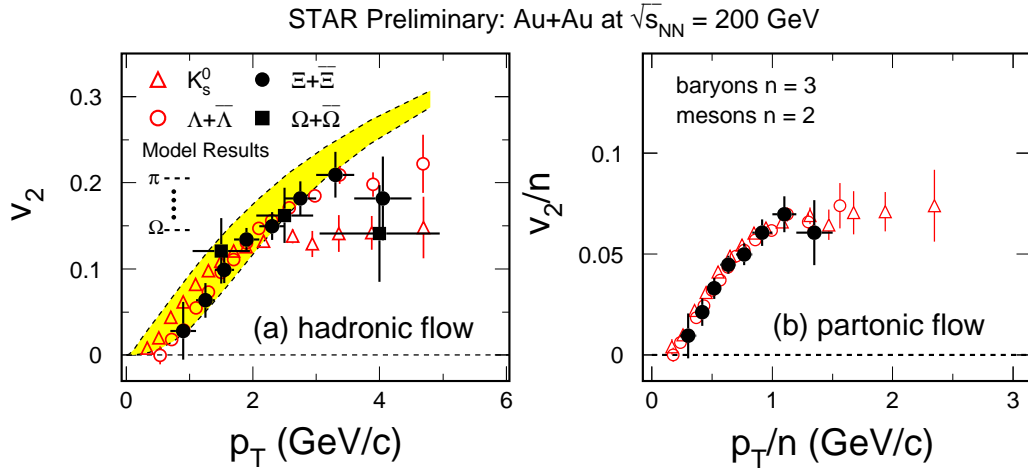


Figure 4. (a) Measured azimuthal anisotropy parameters v_2 of strange hadrons as a function of transverse momentum p_T for minimum bias Au+Au collisions at $\sqrt{s_{NN}}=200$ GeV. The hatched band indicates typical results from hydrodynamical calculations from the pion mass (upper dashed curve) to the Ω mass (lower dashed curve) and (b) azimuthal anisotropy parameters v_2/n versus p_T/n , with n the number of constituent quarks of the corresponding hadron.

The hatched band indicates typical results from hydrodynamical calculations [22] from the pion mass (upper dashed curve) to the Ω mass (lower dashed curve). The calculations describe the experimental data well over a large range in p_T , but systematically overshoot the data at $p_T > 3$ GeV/c. Quark coalescence models predict a universal scaling of elliptic flow parameters versus p_T with the number n of constituent quarks. Figure 4(b) shows our experimental data with v_2 and p_T scaled by n . Our results agree with the predicted scaling within statistical uncertainties. Higher statistics data is needed to further probe quark coalescence models. Of special interest is a high statistics v_2 measurement of ϕ and Ω which will allow for the unambiguous distinction between parton recombination and statistical hadro-chemistry to be the dominant process in hadronization at intermediate p_T [23]. Note, that kaon fusion is unlikely to be the dominant production mechanism of ϕ mesons [24]. Therefore, the ϕ meson might carry dominantly pre-hadronic information. In addition, elliptic flow measurements of the resonances ρ and K^* will offer to disentangle the contribution of partonic and hadronic interactions [25].

STAR also measured directed flow, v_1 [9] and the higher harmonics v_4 and v_6 [26, 27]. For the first time at RHIC, we determined the sign of v_2 to be positive, i.e. in-plane elliptic flow [9].

In addition, we note that two-pion Hanbury Brown–Twiss interferometry relative to the reaction plane indicates that the system at pion kinetic freeze-out is still elongated perpendicular to the reaction plane [28].

5. Bulk properties

Experimental ratios of stable particles have been successfully described within the statistical model using a temperature parameter $T_{ch} = 177 \pm 7$ MeV and a baryo-chemical potential $\mu_b = 29 \pm 6$ MeV in most central Au+Au collisions at $\sqrt{s_{NN}} = 200$ GeV [29, 30]. However, the kinetic freeze-out temperature has been found to be much lower, $T_{kin} = 89 \pm 10$ MeV [30]. Resonances and their hadronic decay daughters might participate in (quasi-)elastic interactions at the late hadronic stage and therefore probe the evolution of the medium until kinetic freeze-out. Figure 5 shows ratios of Δ^{++} , ρ^0 , ϕ , K^* and $\Lambda(1520)$ compared to their corresponding stable particle with identical constituent quark content for Au+Au collisions at $\sqrt{s_{NN}} = 200$ GeV as a function of centrality [31]. All ratios have been normalized to unity for $p + p$ collisions, as indicated by the dashed line. Clearly, the ratios of K^*/K^- and $\Lambda(1520)/\Lambda$ are modified in Au+Au collisions. This indicates that there is an active hadronic stage after chemical freeze-out.

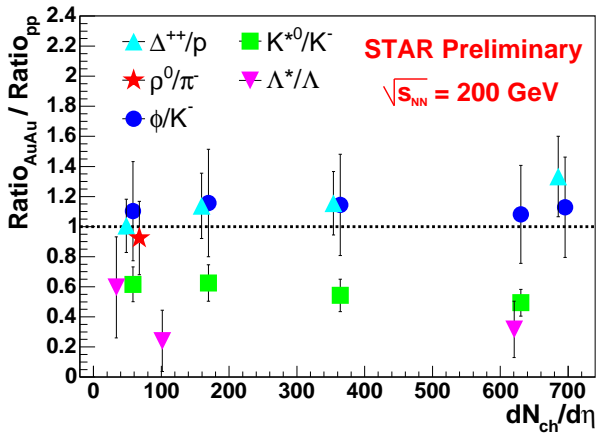


Figure 5. Ratios of resonances compared to their corresponding stable particle with identical constituent quark content for Au+Au collisions at $\sqrt{s_{NN}} = 200$ GeV as a function of centrality. All ratios have been normalized to unity for $p + p$ collisions, as indicated by the dashed line.

6. Heavy Flavor Measurements in $p + p$ and $d+Au$ Collisions

STAR has studied D-meson production at RHIC. D-mesons were identified by calculating the invariant mass of hadronic decay daughter candidates [32] and via electrons(positrons) from semi-leptonic decays [33, 34]. The left hand side of figure 6 shows the invariant yield of D^0 (circles), D^* (squares) and D^\pm (triangles) from $d+Au$ collisions at $\sqrt{s_{NN}} = 200$ GeV as a function of transverse momentum p_T in the range from 0.2 to 11.0 GeV/c . The yields of D^* and D^\pm have been arbitrarily scaled assuming identical spectral shapes of all D-mesons measured. Our experimental yields correspond to a total $c\bar{c}$ production cross section per nucleon–nucleon collision of 1.18 ± 0.21 (stat.) ± 0.39 (syst.) mb. Results from next-to-leading order perturbative QCD calculations [35] predict significantly smaller numbers.

Production of heavy flavor, i.e. charm and beauty was measured in the electron(positron) decay channel. The right hand side of figure 6 shows the invariant yield of summed electrons and positrons [33] as a function of transverse momentum

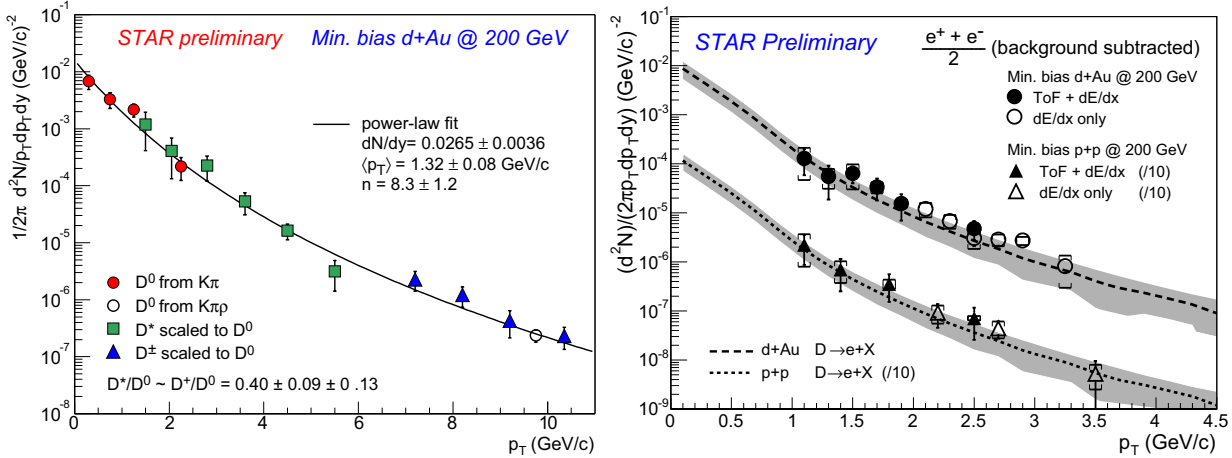


Figure 6. Left: invariant yield of D^0 (circles), D^* (squares) and D^\pm (triangles) from $d+Au$ collisions at $\sqrt{s_{NN}}=200$ GeV as a function of transverse momentum. Right: invariant yield of summed electrons and positrons as a function of transverse momentum from $d+Au$ (upper points) and $p+p$ collisions (lower points). Background from electromagnetic decays has been subtracted. The shaded bands indicate the expected summed electron and positron yield from our D -meson measurements.

p_T from $d + Au$ (upper points) and $p + p$ collisions (lower points). Background from electromagnetic decays has been subtracted. For electron(positron) identification, information on the specific energy loss in the TPC-gas (dE/dx) and time of flight (ToF) was used. The shaded bands indicate the expected electron and positron yield from our D -meson measurement. Within systematic errors of $\approx 30\%$, both measurements are in good agreement. The Barrel Electromagnetic Calorimeter (BEMC) allowed for another independent method of electron(positron) identification [34] up to $p_T < 7$ GeV/c. Decays of B -mesons are expected to dominate the electron(positron) spectrum at $p_T > 5$ GeV/c [34]. All three measurements, namely direct identification of D -mesons by their invariant mass, identifying decay electrons by dE/dx and/or ToF and the BEMC lead to consistent results.

7. Summary

In summary, the suppression of hadron production at intermediate and high p_T in central $Au+Au$ collisions and the $d+Au$ control measurement demonstrate that there are interactions in the medium at the early, most likely partonic stage. As a consequence, bulk matter created at RHIC exhibits strong collective expansion, e.g. large values of elliptic flow. The substantial amount of elliptic flow observed for multi-strange hadrons and the successful description within quark coalescence models suggest that collectivity is indeed built up at the partonic level. We presented first measurements on open charm production at RHIC.

In the future, we need measurements on nuclear modification factors and jet-like correlation of particles carrying heavy flavor ($c-$ and $b-$) quarks to establish microscopic

probes of different mass in order to further characterize the medium created at RHIC. A high statistics elliptic flow measurement of all hadrons, especially ϕ , Ω and the resonances ρ and K^* will enable us to quantify parameters of partonic collectivity and disentangle partonic from hadronic contributions. The ongoing high statistics run at RHIC and our increasingly extending time of flight capabilities as well as an inner μ Vertex detector for heavy-flavor identification which is presently under development will help us in achieving these goals.

- [1] C. Adler *et al.* (STAR Collaboration), Phys. Rev. Lett. **89**, 272302(2002).
- [2] J. Adams *et al.* (STAR Collaboration), subm. to Phys. Rev. Lett.; hep-ex/0310058.
- [3] S. Klein and J. Nystrand, Phys. Rev. Lett. **84**, 2330(2000).
- [4] X.N. Wang and M. Gyulassy, Phys. Rev. Lett. **68**, 1480(1992).
- [5] J. Adams *et al.* (STAR Collaboration), Phys. Rev. Lett. **91**, 172302(2003).
- [6] C. Adler *et al.* (STAR Collaboration), Phys. Rev. Lett. **90**, 032301(2003).
- [7] C. Adler *et al.* (STAR Collaboration), Phys. Rev. Lett. **90**, 082302(2003).
- [8] C. Adler *et al.* (STAR Collaboration), Phys. Rev. Lett. **89**, 202301(2002).
- [9] A. Tang (STAR Collaboration), *these proceedings*.
- [10] F. Wang (STAR Collaboration), *these proceedings*.
- [11] T.A Trainor (STAR Collaboration), Bull. Am. Phys. Soc. **48** 25(2003).
- [12] D. Kharzeev, E. Levin, and L. McLerran, Phys. Lett. **B561**, 93(2003).
- [13] J. Adams *et al.* (STAR Collaboration), Phys. Rev. Lett. **91**, 072304(2003).
- [14] J. Adams *et al.* (STAR Collaboration), Phys. Rev. Lett. **92**, 052302(2004).
- [15] M.A.C. Lamont (STAR Collaboration), *these proceedings*.
- [16] L. Barnby (STAR Collaboration), *these proceedings*.
- [17] D. Molnar and S.A. Voloshin, Phys. Rev. Lett. **91**, 092301(2003).
- [18] R.J. Fries, B. Müller and C. Nonaka, Phys. Rev. Lett. **90** 202303(2003).
- [19] J.-Y. Ollitrault, Phys. Rev. **D46**, 229(1992).
- [20] H. Sorge, Phys. Lett. **B402**, 251(1997).
- [21] J. Castillo (STAR Collaboration), *these proceedings*.
- [22] P. Huovinen *et al.*, Phys. Lett. **B503**, 58(2001).
- [23] C. Nonaka *et al.*, Phys. Lett. **B**, in print; nucl-th/0308051.
- [24] E. Yamamoto (STAR Collaboration), Nucl. Phys. **A715**, 466c(2003).
- [25] C. Nonaka *et al.*, Phys. Rev. **C**, in print; nucl-th/0312081.
- [26] J. Adams *et al.* (STAR Collaboration), Phys. Rev. Lett. **92**, 062301(2004).
- [27] A. Poskanzer (STAR Collaboration), *these proceedings*.
- [28] J. Adams *et al.* (STAR Collaboration), subm. to Phys. Rev. Lett.; nucl-ex/0312009.
- [29] P. Braun-Munzinger, K. Redlich and J. Stachel, nucl-th/0304013.
- [30] J. Adams *et al.* (STAR Collaboration), submitted to Phys. Rev. Lett.; nucl-ex/0310004.
- [31] C. Markert (STAR Collaboration), *these proceedings*.
- [32] A. Tai (STAR Collaboration), *these proceedings*.
- [33] L. Ruan (STAR Collaboration), *these proceedings*.
- [34] A. Suaide (STAR Collaboration), *these proceedings*.
- [35] R. Vogt, hep-ph/0203151.